Anderson transition in a three-dimensional kicked rotor

Jiao Wang

Temasek Laboratories, National University of Singapore, 117542 Singapore
and Beijing-Hong Kong-Singapore Joint Center for Nonlinear and Complex Systems (Singapore),
National University of Singapore, 117542 Singapore

Antonio M. García-García

Physics Department, Princeton University, Princeton, New Jersey 08544, USA
and The Abdus Salam International Centre for Theoretical Physics, P.O.B. 586, 34100 Trieste, Italy

We investigate Anderson localization in a three-dimensional (3D) kicked rotor. By a finite-size scaling analysis we identify a mobility edge for a certain value of the kicking strength $k=k_c$. For $k>k_c$ dynamical localization does not occur, all eigenstates are delocalized and the spectral correlations are well described by Wigner-Dyson statistics. This can be understood by mapping the kicked rotor problem onto a 3D Anderson model (AM) where a band of metallic states exists for sufficiently weak disorder. Around the critical region $k \approx k_c$ we carry out a detailed study of the level statistics and quantum diffusion. In agreement with the predictions of the one parameter scaling theory (OPT) and with previous numerical simulations, the number variance is linear, level repulsion is still observed, and quantum diffusion is anomalous with $\langle p^2 \rangle \propto t^{2/3}$. We note that in the 3D kicked rotor the dynamics is not random but deterministic. In order to estimate the differences between these two situations we have studied a 3D kicked rotor in which the kinetic term of the associated evolution matrix is random. A detailed numerical comparison shows that the differences between the two cases are relatively small. However in the deterministic case only a small set of irrational periods was used. A qualitative analysis of a much larger set suggests that deviations between the random and the deterministic kicked rotor can be important for certain choices of periods. Heuristically it is expected that localization effects will be weaker in a nonrandom potential since destructive interference will be less effective to arrest quantum diffusion. However we have found that certain choices of irrational periods enhance Anderson localization effects.

I. INTRODUCTION

The recent realization of disordered systems by using ultracold atoms [1,2] in optical lattices promises the observation of Anderson localization [3] in three dimensions in the near future. The related concept of dynamical localization [4] has already been observed experimentally [5,6] in one dimension also by using cold atom techniques. The high degree of experimental control on both the residual interactions and the disordered potential make these systems ideal candidates to test the standard theoretical predictions of localization theory [7], namely, exponential localization for any disorder in one and two dimensions and the existence of a metal-insulator transition in more than two dimensions. However for an accurate comparison between experiments and theory it is necessary to take into account that the effective experimental potential is not the simple Gaussian uncorrelated random potential used in theoretical studies. For instance, the potential generated by a speckle pattern [1] is to a good approximation random but highly correlated. In the case of multichromatic [2] optical lattices the effective potential is quasiperiodic rather than random. The one-dimensional (1D) kicked rotor, the model utilized in [5] to study experimentally dynamical localization, is not random either. Its classical dynamics is chaotic so deviations from the predictions of localization theory are expected [8]. In this paper we study similarities and differences between localization effects caused by a truly random potential and the one

associated to a three-dimensional (3D) kicked rotor. Below we review dynamical localization effects in the 1D and 2D kicked rotors and give an overview of the physics of the Anderson transition in 3D disordered systems.

A. Localization in the one-dimensional kicked rotor

The quantum kicked rotor [9,10], namely, a particle in a circle periodically kicked (with period T) by a smooth potential $V(q)=k \cos(q)$,

$$H = \frac{p^2}{2} + V(q) \sum_n \delta(t - Tn), \qquad (1)$$

has played a central role in the development of quantum chaos. This is hardly surprising since, despite its simplicity, it has a very rich and highly nontrivial dynamics. The classical dynamics undergoes a gradual crossover from quasi-integrable to fully chaotic as the kicking strength k is increased. Therefore it is possible to study in detail all types of intermediate behavior between chaos and integrability. Moreover it is specially suitable for numerical simulations since the evolution matrix in a basis of plane waves has a simple form. This was important in the early days of quantum chaos when numerical simulations in conservative 2D chaotic systems were quite expensive.

The quantum dynamics of the kicked rotor is also of interest. For short time scales and k sufficiently large quantum

and classical motion are diffusive. However for longer time scales numerical simulations show [9] that quantum diffusion in momentum space eventually stops, namely, $\lim_{t \to \infty} \langle p^2(t) \rangle$ tends to a constant. By contrast the classical motion is diffusive $\langle p^2(t) \rangle \propto t$. This rather counterintuitive feature, usually referred to as dynamical localization [10], was fully understood [4] after mapping the kicked rotor problem onto a 1D Anderson model (AM) with a pseudorandom potential where localization is well established. In our model the role of the mean free path is played by the kicking strength k. The mapping onto a 1D AM is carried out in two steps: first one writes down the evolution operator U associated with Eq. (1),

$$U = e^{-i\hat{p}^2 T / 2\bar{h}} e^{-iV(\hat{q})/\bar{h}}. \tag{2}$$

In a basis of plane waves, U has matrix elements

$$U_{lm} = (-i)^{l-m} e^{-im^2 T\hbar/2} J_{l-m}\left(\frac{k}{\hbar}\right), \tag{3}$$

where $J_n(k)$ is a Bessel function of first kind. Then a given eigenstate of U with eigenvalue $\exp(-i\omega)$ can be transformed into an effective Hamiltonian problem [4],

$$\mathcal{H}\psi_n = \epsilon_n \psi_n + \sum_m F(m - n)\psi_m \tag{4}$$

where $\epsilon_n = \tan(\omega/2 - \tau n^2/4)$ and

$$F(m - n) = -\frac{1}{2\pi} \int_{-\pi}^{-\pi} dq \tan[V(q)/2]e^{-iq(m-n)}$$

$$\propto \exp(-A|m - n|) \tag{5}$$

with A a decreasing function of k and $\tau = T/\hbar$. This analytical mapping is only valid provided that $\tan V(q)/2$ is a well-defined function for any q. For $V(q) = k \cos q$ this corresponds to the region $k < \pi$. However even for $k > \pi$ the quantum dynamics of the kicked rotor is qualitatively similar to that of a 1D AM with a random potential. For comparison we note that the standard 1D AM heavily used in numerical and analytical studies of localization is given by

$$\mathcal{H}\psi_n = \epsilon_n \psi_n + \psi_{n+1} + \psi_{n-1}, \tag{6}$$

where ϵ_n are independent random numbers extracted from a Gaussian or box distribution. The quantum dynamics of the Hamiltonian equation (6) is well understood [3,7,11]: eigenstates are exponentially localized and quantum diffusion eventually is arrested for any amount of disorder.

Strictly speaking there are important differences between Eq. (6) and Eq. (4). For instance in Eq. (4) the diagonal disorder ϵ_n is deterministic and the hopping is short range, but it is not restricted to nearest neighbors as in Eq. (6). The latter is not really relevant as it is known [12] that exponential localization for all energies and disorder persists provided that the hopping term decays faster than $1/|n-m|$. Potentials in Eq. (1) leading to a decay of $F(m-n) \sim 1/|n-m|$ in Eq. (4) induce a metal-insulator transition even in 1D [12,13].

The nonrandomness of the diagonal disorder in Eq. (4) is, at least superficially, a more serious deviations from Eq. (6).

However in Ref. [8] it was shown that provided τ is an irrational (both conditions are required to make $\epsilon_n \propto \tau n^2$ effectively pseudorandom) not too small and with a sufficiently poor approximation by a rational number the resulting potential was ergodic and to a great extent not very different from a true random potential. This seems to be related to the fact that in the $n \to \infty$ limit all derivatives of ϵ_n with respect to n are not bounded.

For the sake of completeness we mention that (a) only recently [14] a rigorous proof of localization for the original model, Eq. (1), not involving a mapping onto an AM has been obtained; and (b) localization in more general time-dependent potentials has been recently studied in the mathematical literature. The main conclusion [15] is that quantum localization will generally occur provided the potential is both periodic and smooth in time. Similar results were obtained previously in the physics literature [16] by using heuristic arguments and numerical simulation.

B. Localization in the two-dimensional kicked rotor

A natural question to ask is to what extent these results hold in higher dimensions. One of the more striking predictions of localization theory [7,11], corroborated by numerical simulations, is that eigenstates of the 2D version of Eq. (6) are still exponential localized for any disorder and energy. As in the 1D case, quantum diffusion eventually stops as well. However in more than two-dimensions a metal insulator transition occurs for a critical value of the disorder. The critical disorder increases with the spatial dimensionality of the system [3,7,11]. It is thus highly desirable to determine (a) whether it is possible to extend the above mapping to higher dimensions and (b) whether the resulting extension of Eq. (4) still follows the predictions of localization theory despite the potential being nonrandom.

We note that if the two models are still similar higher-dimensional kicked rotors could be used to study experimentally the Anderson transition by using cold atoms techniques. This is specially relevant as experimental detection of localization has proved to be quite elusive. Moreover it is also important to understand in detail how deviations from an ideal random distribution affects the quantum dynamics of the system. After all any realistic random potential will always present some sort of deviation from a given ideal random distribution.

In fact there are already in the literature different propositions to map a generalization of Eq. (1) onto a higher dimensional AM. In Ref. [17] a multifrequency, time-dependent potential

$$V(q) = k \cos(q + \omega_1 t + \omega_2 t) \tag{7}$$

was mapped onto a 3D version of Eq. (4); namely, an AM with short-range hopping and diagonal disorder

$$\epsilon_{n,n_1,n_2} \sim \tan(\tau n^2 + \omega_1 n_1 + \omega_2 n_2), \tag{8}$$

with n, n_1, n_2 integers numbers. A numerical analysis of the quantum diffusion [17] showed that, as in a 3D AM with a truly random potential, the system avoids dynamical localization for $k > k_c$. Recently it has been possible to model this

generalized kicked rotor by using cold atoms in an optical lattice [18]. In agreement with previous results no dynamical localization was observed for $k > k_c$. However the resulting diagonal disorder in the n_1 and n_2 direction is quasiperiodic rather than quasirandom. It is thus unclear whether this type of kicked rotor can be used as an effective model to study a metal-insulator transition induced by disorder. Indeed the value of the critical exponent [19] controlling the divergence of the localization length in generalizations of Eq. (8) with $d \geqslant 3$ frequencies $\omega_1 \ldots \omega_d$ sharply disagrees with numerical results [11,20] of the d-dimensional equivalent of Eq. (6).

Another generalized kicked rotor with potential

$$V(q_1, q_2) = k \cos(q_1) \cos(q_2) \qquad (9)$$

was studied in Ref. [21]. In this case the mapping is onto a 2D AM with short-range hopping and diagonal disorder

$$\epsilon_{n_1, n_2} \sim \tan(\tau_1 n_1^2 + \tau_2 n_2^2), \qquad (10)$$

with n_1, n_2 integers and τ_1, τ_2 irrationals. This diagonal pseudodisorder is a natural extension of the one-dimensional case, Eq. (4), and consequently shares many of the properties of a true random potential. For instance, the dynamical localization occurs for any value of the kicking strength, and the localization length increases exponentially with k.

C. Localization in a three-dimensional disordered potential: The one parameter scaling theory and properties of the three-dimensional metal-insulator transition

In the context of disordered systems the one parameter scaling theory (OPT) [7] provides a valuable framework to understand localization effects. In two and lower dimensions it predicts the exponential localization of the eigenstates and the arrest of diffusion for any amount of disorder [7]. In three and higher dimensions a metal-insulator transition is expected for a critical amount of disorder. Thus for disorder below the critical one the wave functions are extended through the sample. In the opposite limit, wave functions are exponentially localized as in $d \leqslant 2$.

A key concept in this theory is the dimensionless conductance g introduced by Thouless [22]. It is defined as $g = E_T/\Delta$ where, E_T, the Thouless energy, is an energy scale related to the diffusion time to cross the sample and $\Delta \propto 1/L^d$ is the mean level spacing. In the diffusive limit $E_T \propto 1/L^2$ and therefore $g \propto L^{d-2}$. On the other hand if the particle is exponentially localized, $g \propto e^{-L/\xi}$ where ξ is the localization length and L is the system linear size.

With this simple input it is possible to analyze localization effects in 3D. For a metal $\lim_{L \to \infty} g(L) \to \infty$ and for an insulator $\lim_{L \to \infty} g(L) \to 0$. Since $g(L)$ is continuous and monotonous, the metal-insulator transition is characterized by a size-independent conductance $g = g_c$. This scale invariance together with $\Delta \propto 1/L^3$ leads to a Thouless energy that scales as $E_T \propto 1/L^3$. This only can happen if the diffusion is anomalous at the transition with

$$\langle r^2 \rangle \sim t^{2/3}. \qquad (11)$$

Anomalous diffusion is one of the main predictions of the OPT about the metal-insulator transition.

Additional information about the transition comes mainly from numerical calculations [20]. Level statistics [23,24] are intermediate between those of a metal and those of an insulator. For instance level repulsion is observed as in a disordered metal. By contrast long-range spectral correlations such as the spectral rigidity $\Delta_3(\Lambda)$ are closer to that of an insulator [25,26]. For $\Lambda \gg 1$,

$$\Delta_3(\Lambda) = \frac{2}{\Lambda^4} \int_0^\Lambda (\Lambda^3 - 2\Lambda^2 x + x^3) \Sigma^2(x) dx \sim \chi \Lambda/15,$$

where $\chi < 1$ at the metal insulator transition and $\chi = 1$ for an insulator; Λ is a spectral window containing Λ eigenvalues in units of the mean level spacing Δ; $\Sigma^2(\Lambda) = \langle N_\Lambda^2 \rangle - \langle N_\Lambda \rangle^2$ is the number variance (N_Λ is the number of eigenvalues in an interval of length Λ).

The critical exponent controlling the divergence of the localization length at the transition is supposed to be a decreasing function of the space dimensionality. In 3D it is approximately given by $\nu \approx 3/2$ [20]. Recently one of us showed [25] that some of these features can be obtained analytically by combining the OPT with the self-consistent theory of localization [27]. A natural question to ask is to what extent these results hold if the potential is not completely random. The main aim of this paper is to answer this question.

D. Organization of the paper

We study a 3D kicked rotor with

$$V(q_1, q_2, q_3) = k \cos(q_1) \cos(q_2) \cos(q_3). \qquad (12)$$

It will be shown that this model maps onto a 3D version of Eq. (4) with short-range hoping and an on-site potential that shares many quasirandom features of the 1D and 2D cases.

By a careful finite-size scaling analysis it will show that this model undergoes a metal-insulator transition at a certain kicking strength $k = k_c$. For technical reasons we have investigated in detail only a small sets of irrational periods $\{\tau_i\}$ with $i = 1, 2, 3$. Within this set the numerical value of k_c depends weakly on the $\{\tau_i\}$. Dynamical localization consequently only occurs for $k < k_c$. We then study in detail level statistics and quantum diffusion in the critical region $k \approx k_c$. In agreement with previous numerical results of the level statistics of the 3D AM at the transition, we have found that (a) the spectral rigidity is linear; (b) as in a metal, level repulsion is still observed; (c) as in an insulator, the asymptotic decay of the level spacing distribution is exponential. Moreover, in agreement with the one parameter scaling theory (OPT), the diffusion is anomalous at the transition with $\langle p^2 \rangle \propto t^{2/3}$.

Finally we investigate to what extent Anderson localization is affected by the pseudorandom nature of the potential. In order to proceed we compare the results of previous sections with those coming from a 3D kicked rotor in which the phase of the kinetic term of the evolution matrix is random. The main differences between the random and pseudorandom cases are as follows: (a) the critical kicking strength k_c is slightly larger ($k_c \sim 2.4$ versus $k_c \sim 2.3$) than in the random

case; (b) the slope of the spectral rigidity is smaller in the random case; c) statistical fluctuations are much stronger in the pseudorandom case. These results are consistent with the heuristic picture that localization will be stronger the more random and/or uncorrelated the potential is (for additional references about different ways to measure differences between a random and a pseudorandom potential we refer to [28]). However a qualitative analysis of a much larger set of $\{\tau_i\}$ suggests that deviations between the random and the deterministic kicked rotor can be important for certain choices of periods. Contrary to intuition certain choices of $\{\tau_i\}$ can enhance Anderson localization effects and lead to a larger k_c than in the random case.

II. CALCULATION OF THE CRITICAL STRENGTH k_c AND CRITICAL EXPONENT ν

We study the quantum dynamics of a 3D kicked rotor with a smooth potential,

$$\mathcal{H} = \frac{1}{2}(\tau_1 p_1^2 + \tau_2 p_2^2 + \tau_3 p_3^2) + V(q_1, q_2, q_3)\sum_n \delta(t-n) \tag{13}$$

with

$$V(q_1, q_2, q_3) = k\cos(q_1)\cos(q_2)\cos(q_3), \tag{14}$$

$T = \hbar \equiv 1$, τ_1, τ_2, τ_3 are irrational numbers not too close to any rational multiple of π. It is important to choose $\{\tau_i\}$ in such a way that correlations caused by the proximity to a rational number are suppressed. However it is hard to quantitatively assess how the specific choice of $\{\tau_i\}$ will influence Anderson localization effects. In 3D this is rather a number theory problem which is beyond the scope of this paper. Here in order to qualitatively address this issue we have employed the following two different methods to generate a given set of $\{\tau_i\}$:

Method 1. We set $\tau_1 = \alpha/\lambda^2$, $\tau_2 = \alpha/\lambda$, and $\tau_3 = \alpha$, where $\lambda = 1.3247\ldots$ is the real root of the equation $\lambda^3 - \lambda - 1 = 0$, and α is a random number extracted from a box distribution with support (10,20). In this way $\tau_i \gg 1$. This is a necessary condition in order to have pseudorandom features. A given α is only accepted if the resulting continuous fraction form of τ_1/π, τ_2/π and τ_3/π specified by a sequence of integers, say, $[a_1, a_2, \ldots]$ is such that the maximum value of $|a_i|$ is smaller than 12. This is enough to prevent the system to be close to a quantum resonance. We note that the smaller these integers a_i are the more irrational are τ_i/π.

Method 2. We set $\tau_1 = \alpha/\sigma$, $\tau_2 = \alpha$, and $\tau_3 = \sigma\alpha$, where $\sigma \approx 1.618$ is the golden mean. Then we follow method 1.

In this section we carry out a finite-size scaling analysis in order to determine the impact of this type of pseudorandomness on Anderson localization effects. We will show that the system undergoes a metal insulator transition at $k = k_c = 2.27 \pm 0.07$ if method 1 is used and $k = k_c = 2.35 \pm 0.10$ if method 2 is used. By contrast if the phase of the kinetic term of the evolution matrix is completely random (see last section) $k_c = 2.40 \pm 0.05$. It thus clear that the pseudorandom nature of the $\{\tau_i\}$ have a sizable but small effect on the local-

ization transition. We shall see in the last section that for certain choices of $\{\tau_i\}$ these differences can be much larger and likely lead to k_c quite different from the one corresponding to the random case.

In order to proceed we evaluate the quantum evolution operator U. After a period $T \equiv 1$ (we remember that $\hbar \equiv 1$), an initial state ψ_0 evolves to

$$\psi(1) = U\psi_0 = e^{-i\hat{p}^2/2}e^{-iV(\hat{q})}\psi_0, \tag{15}$$

where $\hat{p}$ and $\hat{q}$ stand for the usual momentum and angular position operator. We then express the evolution operator U in a basis of the momentum eigenstates,

$$\langle\mathbf{m}|U|\mathbf{n}\rangle = \frac{1}{N}e^{-i(\tau_1 n_1^2 + \tau_2 n_2^2 + \tau_3 n_3^2)/2}\sum_{\mathbf{l}}e^{i\phi(\mathbf{l}, \mathbf{m}, \mathbf{n})}, \tag{16}$$

where $\langle\mathbf{q}|\mathbf{n}\rangle = \frac{e^{i\mathbf{n}\cdot\mathbf{q}}}{(2\pi)^{3/2}}$ with $\mathbf{q} = (q_1, q_2, q_3)$, $\mathbf{n} = (n_1, n_2, n_3)$, $\phi(\mathbf{l}, \mathbf{m}, \mathbf{n}) = 2\pi(\mathbf{l} + \boldsymbol{\theta})(\mathbf{m} - \mathbf{n})/N - V[2\pi(\mathbf{l} + \boldsymbol{\theta})/N]$, $\mathbf{l} = (l_1, l_2, l_3)$, $l_i = -N/2, \ldots, N/2 - 1$. Here N^3 specifies the dimension of the Hilbert space. We restrict ourselves to even N throughout this work. The parameter $\boldsymbol{\theta} \equiv (\theta_1, \theta_2, \theta_3)$ depends on the boundary conditions $0 \leq \theta_i \leq 1$. We set $\boldsymbol{\theta} = \mathbf{0}$ that corresponds to periodic boundary conditions. With this choice our system is time reversal invariant. For the effect of the breaking of time reversal symmetry on localization effects we refer to [29].

The eigenvalues and eigenvectors of U can now be computed by using standard diagonalization techniques. The eigenvalues of the evolution matrix are the starting point to carry out the finite-size scaling analysis.

Finally we note that following the procedure of Ref. [4] it is possible to map a given eigenstate of U with eigenphase $e^{i\omega}$ onto a 3D AM,

$$\mathcal{H}\psi_{\mathbf{n}} = \epsilon_{\mathbf{n}}\psi_{\mathbf{n}} + \sum_{\mathbf{m}}F(\mathbf{m} - \mathbf{n})\psi_{\mathbf{m}} \tag{17}$$

where

$$\epsilon_{\mathbf{n}} = \tan(\omega/2 - \tau_1 n_1^2/4 - \tau_2 n_2^2/4 - \tau_3 n_2^2/4) \tag{18}$$

and

$$F(\mathbf{m} - \mathbf{n}) = -\frac{1}{(2\pi)^3}\int_{-\pi}^{-\pi}d^3q \tan[V(\mathbf{q})/2]e^{-i\mathbf{q}(\mathbf{m}-\mathbf{n})}$$

$$\propto \exp(-A|\mathbf{m} - \mathbf{n}|)$$

with A a decreasing function of the kicking strength. The form of the diagonal disorder and hopping is similar to the 1D case. We thus expect that the quantum dynamics of Eq. (17) is qualitatively similar to that of a 3D AM with uncorrelated disorder and hopping restricted to nearest neighbors. However deviations are expected since the potential, Eq. (18), have strong correlations (see Fig. 5).

Our first task is to find out the critical k_c and the critical exponent ν associated with the divergence of the localization length at the transition. In order to proceed we determine k_c by using the finite-size scaling method [23]. First we evaluate a certain spectral correlator for different sizes N and disorder strengths k. Then we locate the transition by finding the kicking strength k_c such that the chosen scaling variable be-
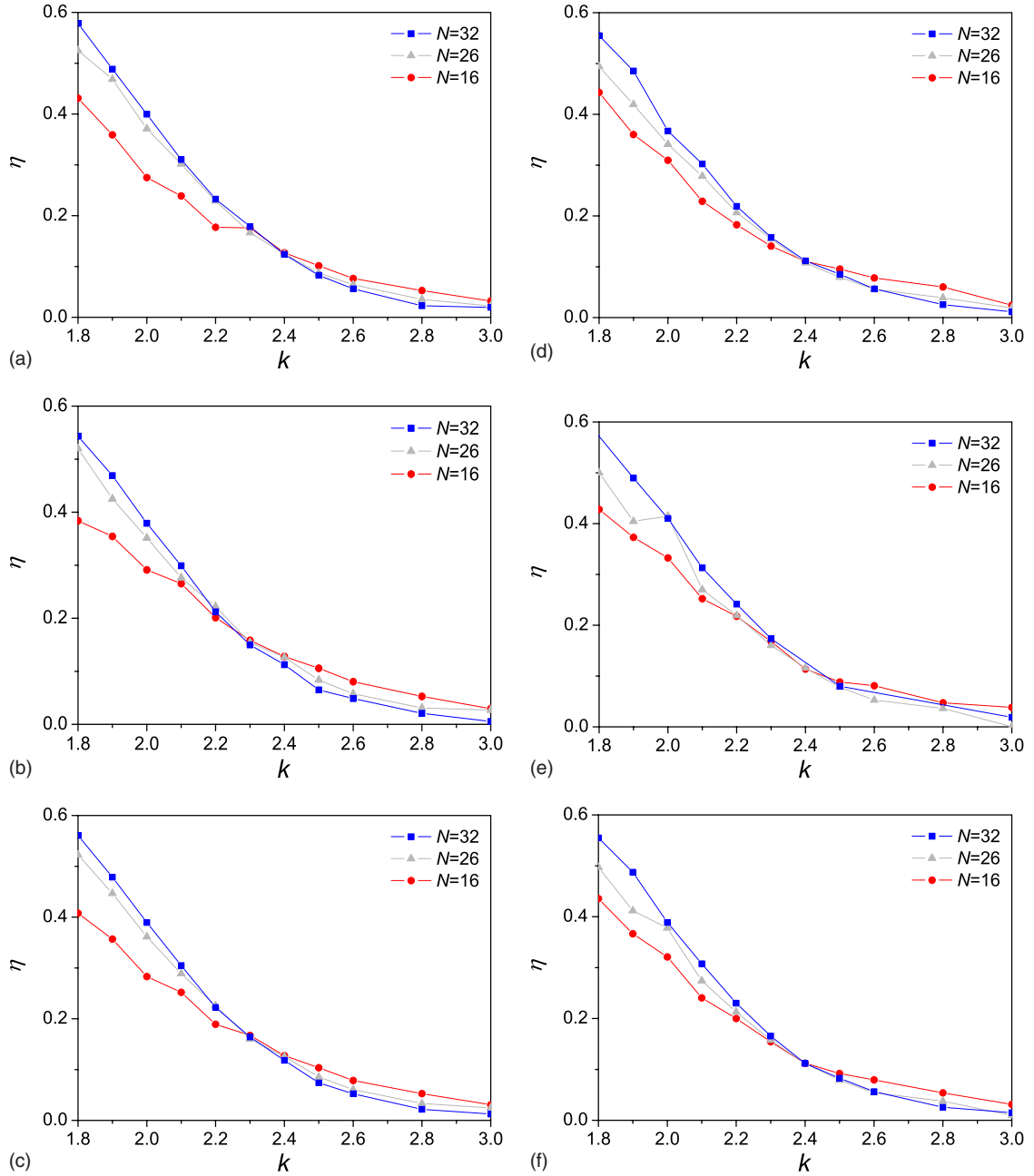
FIG. 1. (Color online) Scaling variable η given by Eq. (19) as a function of k for different system sizes N. Plots (a) and (b) show results for two different sets of $\{\tau_i\}$ generated by following method 1 (see text) with $\alpha \approx 18.155\,757\,057\,050\,607\,1$ (a) and $\alpha \approx 18.532\,836\,635\,266\,9$ (b). Plot (c) shows the averaged results of (a) and (b). The finite-size scaling analysis suggests that a metal-insulator transition occurs at $k_c = 2.27 \pm 0.07$ with a critical exponent $\nu = 1.61 \pm 0.25$. Plots (d), (e), and (f) are the equivalent of plots (a), (b), and (c) but with $\{\tau_i\}$ obtained by method 2 with $\alpha \approx 17.213\,926\,316\,790\,2$ (d) and $\alpha \approx 13.319\,552\,392\,774\,2$ (e) instead. In this case we obtain $k_c = 2.35 \pm 0.1$ with $\nu = 1.67 \pm 0.27$.

comes size independent. In our case we investigate the level spacing distribution $P(s)$ [30] [probability of finding two neighboring eigenvalues at a distance $s = (\epsilon_{i+1} - \epsilon_i)/\Delta$, with Δ being the local mean level spacing]. In order to avoid any dependence on bin size, the scaling behavior of $P(s)$ is examined through the following function of its variance [31]:

$$\eta(N, W) = [\mathrm{var}(s) - \mathrm{var_{WD}}]/[\mathrm{var_P} - \mathrm{var_{WD}}]. \qquad (19)$$

In Eq. (19) $\mathrm{var}(s) = \langle s^2 \rangle - \langle s \rangle^2$, where $\langle \cdots \rangle$ denotes spectral

averaging over a single set of $\{\tau_i\}$. $\mathrm{var_{WD}} \approx 0.286$ and $\mathrm{var_P} = 1$ are the variances of Wigner-Dyson (metal) and Poisson (insulator) statistics [30], respectively. Hence $\eta = 1(0)$ for an insulator (metal). Any other intermediate value of η in the $N \rightarrow \infty$ limit is an indication of a metal-insulator transition.

In Fig. 1 we plot the k dependence of η for different system sizes. The critical disorder $k = k_c$ signaling the Anderson transition corresponds to the point for which η is independent of N. For a smaller (larger) k, η tends to the insula-

tor (metal) prediction. For a precise determination of the critical k_c and the critical exponent ν we look at the correlation length near k_c,

$$\xi(k) = \xi_0 |k - k_c|^{-\nu}, \qquad (20)$$

where ξ_0 is a constant. The numerical values of k_c and ν are obtained by expressing $\eta(N,k) = f[N/\xi(k)]$ and then performing an expansion around the critical point

$$\eta(N,k) = \eta_c + \sum_n C_n (k - k_c)^n N^{n/\nu}. \qquad (21)$$

In practice, we have truncated the series at $n=2$ and then we have performed a statistical analysis of the data with the Levenberg-Marquardt method for nonlinear least-squares models. The most likely fit is determined by minimizing the χ^2 statistics of the fitting function (21). We found $k_c = 2.27 \pm 0.07$ with $\nu = 1.61 \pm 0.25$ for method 1 and $k_c = 2.35 \pm 0.1$ with $\nu = 1.67 \pm 0.27$ for method 2. The numerical value of ν is higher but quite close to the one found in the 3D AM at the transition $\nu \approx 1.5$. We stress that these results were obtained with only the data of Fig. 1, namely, an average over only two sets of $\{\tau_i\}$ for each method.

Heuristically it is expected that localization effects will be weaker in a nonrandom potential since destructive interference will be less effective to arrest the quantum motion. Our results are thus consistent with this picture. We note that this conclusion (see next section) might be misleading due to the small number of $\{\tau_i\}$ utilized. Indeed in the final section we shall see that our results are typical, namely, for the majority of $\{\tau_i\}$ we shall get similar results. However there are some choices of irrational $\{\tau_i\}$ that can lead to larger deviations from the results presented in this section.

III. LEVEL STATISTICS

As was mentioned previously the analysis of level statistics is a powerful tool to investigate the metal-insulator transition. At the transition level statistics are intermediate between that of a metal and that of a insulator. For instance, (a) $P(s) \sim s$ for $s \ll 1$, a typical feature of a disordered metal, is still observed at the transition; (b) $\Delta_3(\Lambda) = \chi \Lambda/15$ for $\Lambda \gg 1$ with $\chi < 1$ [20,24–26,32]. This is similar to the result for an insulator $\Delta_3(\Lambda) = \Lambda/15$; c) likewise $P(s) \propto e^{-As}$ with $s \gg 1$ and $A > 1$. For an insulator $P(s) = e^{-s}$.

We explore to what extent these features are also observed in our 3D kicked rotor. As is shown in Fig. 2, qualitatively the level statistics of the eigenphases of the evolution matrix at $k \approx k_c$ are strikingly similar to those of a 3D AM at the transition. The spectral rigidity $\Delta_3(\Lambda)$ is linear, there is level repulsion for $s \ll 1$, the spectrum is scale invariant and $P(s)$ decays exponentially for $s \gg 1$. The slope of $\Delta_3(\Lambda)$, $\chi \approx 0.29$ in our case, is larger than the one corresponding to a random kinetic term (see next section). This suggests that the quasirandom nature of our model only modifies quantitatively, nonqualitatively, the transition. As was expected, level statistics in the limits $k \gg (\ll) k_c$ are described by Wigner-Dyson (Poisson) statistics typical of a metal (insulator). We note that for systems with time reversal invariance the Wigner-Dyson statistics is usually defined by the spectral
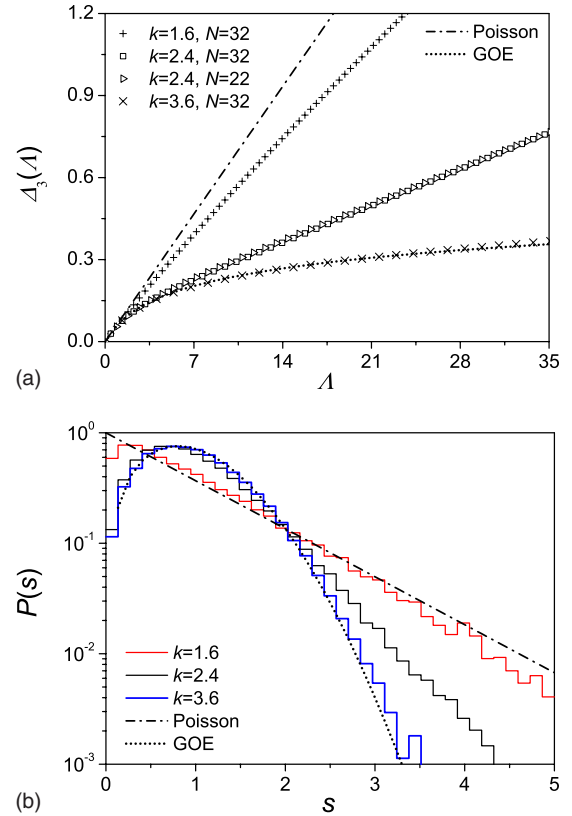

(a)

(b)

FIG. 2. (Color online) The spectral rigidity $\Delta_3(\Lambda)$ and level spacing distribution $P(s)$ for three different kicking values, above, below, and close to the transition $k_c \approx 2.4$ in the 3D kicked rotor, Eq. (13), with $\{\tau_i\}$ the same as in Fig. 1(a). A transition from Poisson to Wigner-Dyson statistics for a system with time reversal invariance (GOE) is clearly observed as the kicking strength crosses the critical value $k \approx k_c$ from below. For $k \approx k_c$ the level statistics have all the signatures of a metal-insulator transition such as (a) an asymptotically linear $\Delta_3(\Lambda) \sim \chi L/15$ with $\chi \sim 0.29$, (b) level repulsion for $s \to 0$ as in a metal $[\lim_{s\to 0} P(s) = 0]$, and (c) exponential decay of $P(s)$ for $s \gg 1$ as in an insulator. In agreement with the OPT, level statistics are scale invariant for $k \approx k_c$.

properties of the Gaussian orthogonal ensemble of random matrices (GOE).

IV. QUANTUM DIFFUSION

We now study quantum diffusion in the region $k \approx k_c$. Our motivation is to find out whether the predictions of the scaling theory still hold in the 3D kicked rotor, Eq. (13).

Provided that the classical phase is fully chaotic we expect the classical motion to be diffusive $\langle \Delta p^2(t) \rangle \propto t$. By contrast quantum dynamics depends strongly on k. In analogy with a prediction of the OPT for the 3D AM, we expect dynamical localization for $k < k_c$. In the opposite limit, quantum effects are small, dynamical localization is avoided, and diffusion does not stop though it might slow down as a consequence of interference effects.

According to the OPT (see the Introduction) for $k \approx k_c$, quantum diffusion must be anomalous $\langle \Delta p^2(t) \rangle \propto t^{2/3}$. In Fig. 3, we show the classical and quantum $\langle \Delta p^2(t) \rangle$ for different
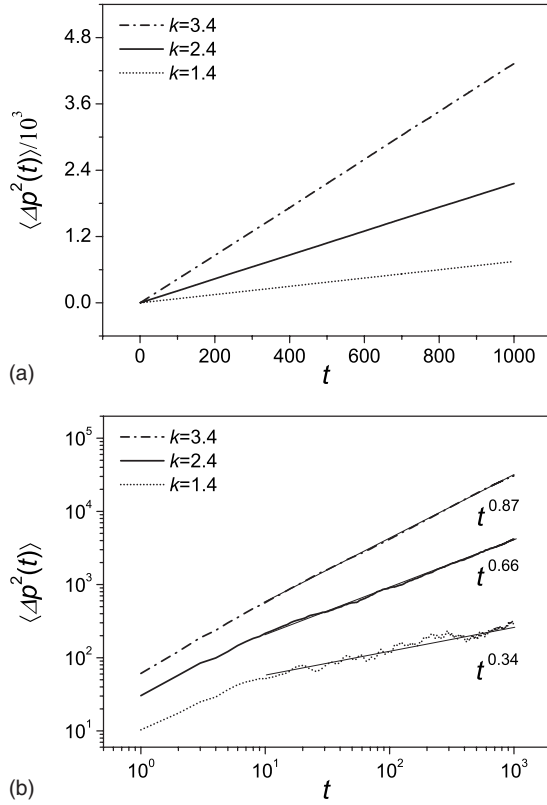
FIG. 3. Classical (a) and quantum (b) diffusion, $\langle \Delta p^2(t) \rangle$ $\equiv \langle [p(t) - p(0)]^2 \rangle$, for three different kicking values, above, below, and close to the transition $k_c \approx 2.4$ in the 3D kicked rotor, Eq. (13), with $\{\tau_i\}$ as in Fig. 1(a). Classical diffusion is normal for the three kicking values however interference effects slows down and eventually arrests quantum diffusion for $k < k_c$. In agreement with OPT $\langle p^2 \rangle \propto t^{2/3}$ at $k \approx k_c$. Thin solid lines in (b) are the best fits in the window $10 < t < 1000$.

values of the kicking strength. We find full agreement with the predictions of the OPT: dynamical localization is avoided for $k > k_c$ and, for $k \approx k_c$, diffusion is anomalous with $\langle \Delta p^2(t) \rangle \propto t^\beta$, $\beta \approx 0.66$. We note that the determination of k_c using the finite-size scaling method is fully consistent with the results from quantum diffusion.

The classical $\langle \Delta p^2(t) \rangle$ was computed by averaging over an ensemble of 10^6 initial ($t=0$) states uniformly distributed in $-\pi < q_i(0) < \pi$ with $p_i(0) = 0$; $i = 1, 2, 3$. In the quantum case we average over the following four initial conditions, $|\mathbf{n}\rangle = |0,0,0\rangle$, $|0,0,1\rangle$, $|0,1,0\rangle$, and $|1,0,0\rangle$.

V. EFFECT OF CORRELATIONS: COMPARISON WITH A 3D KICKED ROTOR WITH A RANDOM KINETIC TERM

In this section we compare previous results with those coming from a 3D kicked rotor similar to Eq. (13) but with the kinetic term of the evolution matrix completely random, namely the factor $e^{i(\tau_1 n_1^2 + \tau_2 n_2^2 + \tau_3 n_3^2)}$ is replaced by $e^{i\phi}$ where ϕ is a random number in $[0, 2\pi)$.

Our motivation is to clarify to what extent the deterministic but pseudorandom character of the motion of the 3D
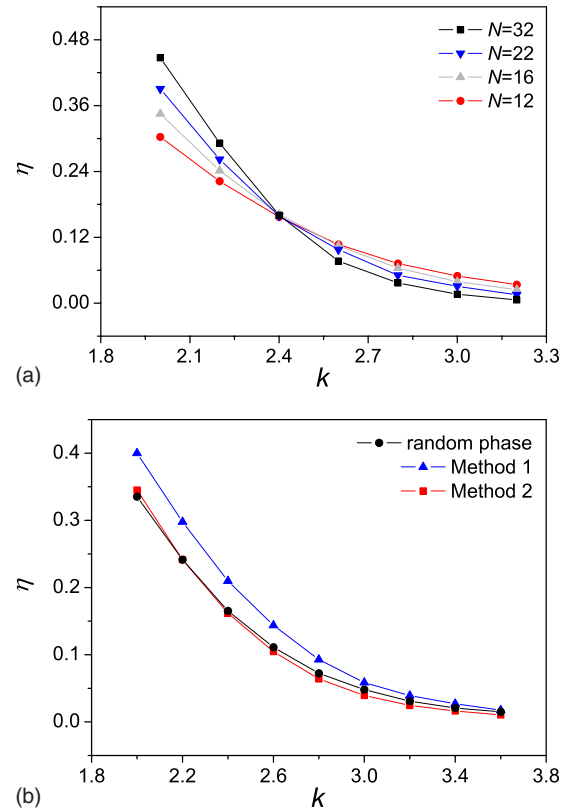

FIG. 4. (Color online) (a) η versus the kicking strength for different system sizes N for a 3D kicked rotor in which the phase of the kinetic term of the evolution matrix is random (see text). A transition is again observed but for a slightly bigger $k_c = 2.4 \pm 0.05$. (b) η for a randomized 3D kicked rotor (random phase plot) and for the deterministic kicked rotor of Eq. (13) with $\{\tau_i\}$ chosen from the two methods mentioned in the text. In both cases $N = 16$. Small but sizable differences are clearly observed specially in the insulator region. For these $\{\tau_i\}$ correlations in the deterministic 3D kicked rotor seem to slightly weaken localization effects. In order to a meaningful comparison in the deterministic case we carry out a full ensemble average over 1280 sets of $\{\tau_i\}$.

kicked rotor, Eq. (13), weakens Anderson localization effects. This is relevant for applications as in realistic situations where it is hard to produce a truly random potential free from correlations. In essence we repeat the calculations of the previous section but for the randomized version of the 3D kicked rotor: (a) we carry out a finite-size scaling analysis to determine k_c and ν (see Fig. 4), (b) we compute the spectral rigidity and level spacing distribution in the metallic, critical, and insulator region, (c) we study quantum diffusion for $k \approx k_c$.

The main conclusions are as follows:

(a) A transition is also observed in this model but at a slightly greater $k \approx k_c = 2.4$ than in the deterministic case (see Fig. 4).

(b) The slope of the number variance $\chi \approx 0.22$ is smaller than in the deterministic case. This is consistent with weaker localization effects in the deterministic case.

(c) $\nu \approx 1.6 \pm 0.2$ is roughly the same in both cases. This is expected as the numerical value of critical exponents should not depend on the microscopic details of the system.
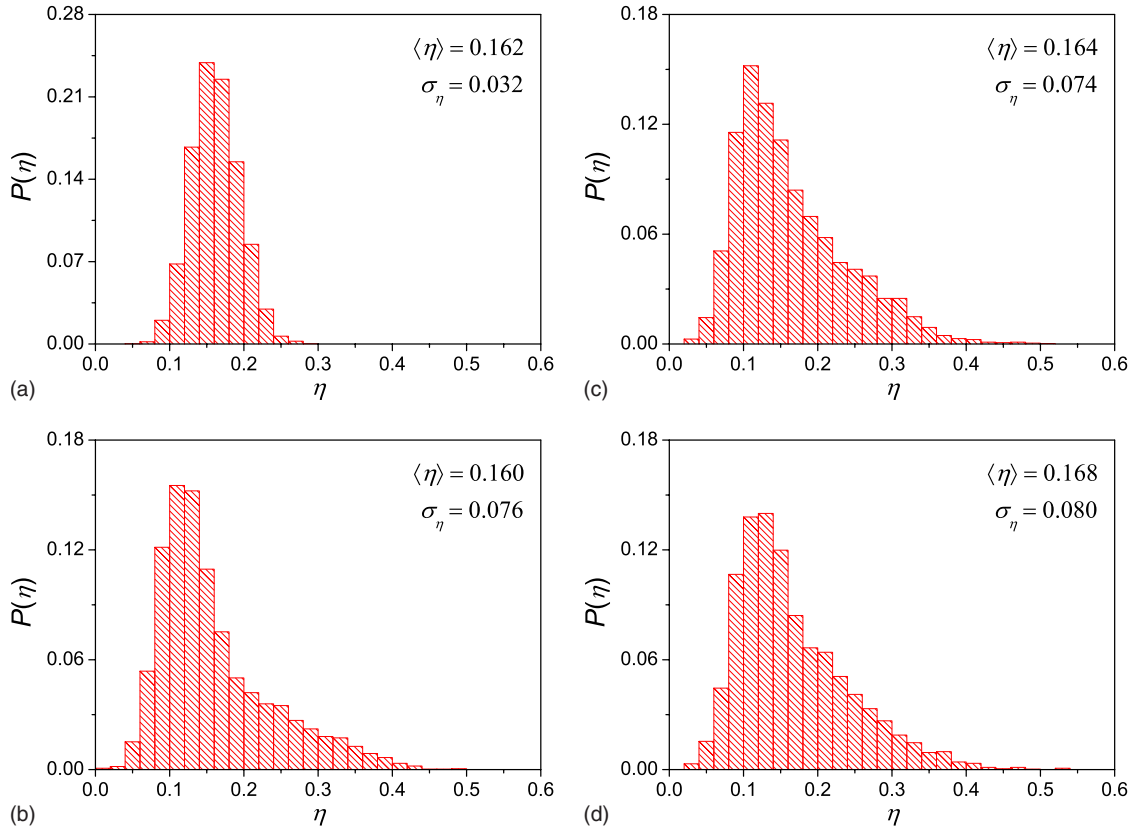
FIG. 5. (Color online) Distribution of η for a 3D kicked rotor, Eq. (13), with (a) the kinetic term replaced by a random phase, (b) $\{\tau_i\}$ given by method 1, (d) $\{\tau_i\}$ given by method 2, and (c) the same for method 2 but where the integer sequence $[a_1, a_2, \ldots]$ for the continuous fraction form of τ_i/π satisfies $|a_i| < 9$ instead. In all cases 1280 sets of $\{\tau_i\}$ are considered and $N=16$.

(d) Quantum diffusion is anomalous with $\langle p^2(t) \rangle \propto t^{2/3}$ and virtually indistinguishable from both the deterministic and the 3D AM. This together with the scale invariance of the spectral correlations, the level repulsion, the asymptotic linear behavior of the spectral rigidity and the numerical value of critical exponent ν seem to be the more robust features of the transition.

A remark is in order. The results for the random case were obtained by performing an ensemble average over 1280 different realizations. By contrast in the deterministic case we did not want to perform an artificial ensemble average so the results presented corresponds to only a handful of different $\{\tau_i\}$.

A natural question to ask is to what extent the numerical values of k_c will be different if other $\{\tau_i\}$ would have been used. For the $\{\tau_i\}$ used here we have obtained a k_c which is slightly smaller than in the random case. By contrast in a recent paper [33] we found $k_c \approx 3.3$ and $\eta_c \approx 0.06$ for $\tau_1 = 1$, $\tau_2 = 1/\lambda$, and $\tau_3 = 1/\lambda^2$ with lambda the root of $x^3 - x - 1 = 0$. This value of k_c is sizable larger than the one $k_c \approx 2.4$ found in the random case. This suggests that for that choice of $\{\tau_i\}$ the effect of correlations enhances localization effects. Several questions then arise: what is the probability that a given set of periods $\{\tau_i\}$ leads to an enhancement and/or suppression of localization? On average, what is the magnitude of the typical deviations from the random case?

Unfortunately a detailed answer to these questions faces technical difficulties as the finite-size scaling method is quite expensive numerically. Moreover, on a more fundamental level, this is rather a number theory problem that, as far as we know, has not yet been tackled in the mathematical literature.

In order to give a qualitatively answer to these questions we compute the full distribution of η, its average $\langle \eta \rangle$ and standard deviation σ_η where $\langle \ldots \rangle$ stands for spectral and ensemble average (see Fig. 5). In the deterministic case we carry the ensemble average over different sets of $\{\tau_i\}$: from method 1, method 2, and method 2 but with $|a_i| < 9$. In each case 1280 different choices of $\{\tau_i\}$ are considered. In the random case the average is carried out also over 1280 different random realizations as it is explained above. Several conclusions can be extracted from this numerical calculation (see Fig. 5): (a) The distribution in the random case is much narrower than in the deterministic case and as a consequence the standard deviation is much smaller. It is thus expected that specific choices of $\{\tau_i\}$ could lead to sizable deviations between the random and deterministic case. (b) The distribution of η for the different methods of obtaining $\{\tau_i\}$ are qualitatively similar. That suggests that provided that $\{\tau_i\}$ is sufficiently irrational ($|a_i| < 12$) the distribution of η is not very sensitive to the way in which $\{\tau_i\}$ is generated. (c) The distribution of η is clearly asymmetric. A longer tail is observed in the region of greater η which indicates that for a sizable percentage of $\{\tau_i\}$ localization effects are considerably suppressed. At the same time the maximum of the distribution is slightly shifted to the left with respect of the random case.

Therefore for a typical $\{\tau_i\}$, k_c will be somehow smaller than in the random case and consequently localization effects will be mildly suppressed due to the nonrandom character of the motion.

VI. CONCLUSIONS

We have studied the quantum dynamics of a 3D kicked rotor with a smooth potential. A careful finite-size scaling analysis has shown that this system undergoes a metal-insulator transition for $k \approx k_c$. The value of k_c barely depends on the numerical choice of $\{\tau_i\}$ provided it is sufficiently irrational. By sufficiently irrational we mean that the continuous fractional decomposition of τ_i in terms of the integers a_i is such that the maximum a_i is less than 12. However from the analysis of the distribution of η it is likely that for particular choices of irrational $\{\tau_i\}$ stronger deviations are observed.

In the critical region $k \approx k_c$ we have investigated in detail quantum diffusion, level statistics, and critical exponents. It has been shown that quantum diffusion, in agreement with the prediction of the OPT, is quantitatively similar to that of a 3D AM at the transition. Typical signatures of a metal-insulator transition such as a linear spectral rigidity or level repulsion have also been observed in our 3D kicked rotor for both deterministic and random kinetic terms.

[1] L. Sanchez-Palencia D. Clement, P. Lugan, P. Bouyer, G. V. Shlyapnikov, and A. Aspect, Phys. Rev. Lett. **98**, 210401 (2007); J. Billy *et al.*, Nature (London) **453**, 891 (2008).

[2] G. Roati *et al.*, Nature (London) **453**, 895 (2008).

[3] P. W. Anderson, Phys. Rev. **109**, 1492 (1958).

[4] S. Fishman, D. R. Grempel, and R. E. Prange, Phys. Rev. Lett. **49**, 509 (1982); D. L. Shepelyansky, *ibid.* **56**, 677 (1986).

[5] F. L. Moore, J. C. Robinson, C. F. Bharucha, B. Sundaram, and M. G. Raizen, Phys. Rev. Lett. **75**, 4598 (1995).

[6] H. Ammann, R. Gray, I. Shvarchuck, and N. Christensen, Phys. Rev. Lett. **80**, 4111 (1998); B. G. Klappauf, W. H. Oskay, D. A. Steck, and M. G. Raizen, *ibid.* **81**, 4044 (1998); M. B. d'Arcy, R. M. Godun, M. K. Oberthaler, D. Cassettari, and G. S. Summy, *ibid.* **87**, 074102 (2001); J. Gong, H. J. Worner, and P. Brumer, Phys. Rev. E **68**, 056202 (2003).

[7] E. Abrahams, P. W. Anderson, D. C. Licciardello, and T. V. Ramakrishnan, Phys. Rev. Lett. **42**, 673 (1979).

[8] D. R. Grempel, R. E. Prange, and S. Fishman, Phys. Rev. A **29**, 1639 (1984); R. Blümel, R. Meir, and U. Smilansky, Phys. Lett. **103A**, 353 (1984).

[9] G. Casati, B. V. Chirikov, J. Ford, and F. M. Izrailev, in *Stochastic Behavior in Classical and Quantum Hamiltonian Systems*, edited by G. Casati and J. Ford, Lecture Notes in Physics Vol. 93 (Springer-Verlag, Berlin, 1979), p. 334; B. V. Chirikov, F. M. Izrailev and D. L. Shepelyansky, Sov. Sci. Rev., Sect. C, Math. Phys. Rev. **2**, 209 (1981); B. V. Chirikov, Phys. Rep. **52**, 263 (1979); T. Hogg and B. A. Huberman, Phys. Rev. Lett. **48**, 711 (1982).

[10] F. M. Izrailev, Phys. Rep. **196**, 299 (1990).

[11] B. Kramer and A. MacKinnon, Rep. Prog. Phys. **56**, 1469 (1993).

[12] A. D. Mirlin, Y. V. Fyodorov, F. M. Dittes, J. Quezada, and T. H. Seligman, Phys. Rev. E **54**, 3221 (1996); Y. V. Fyodorov and A. D. Mirlin, Phys. Rev. Lett. **67**, 2405 (1991); E. Cuevas, M. Ortuno, V. Gasparian, and A. Perez-Garrido, *ibid.* **88**, 016401 (2001).

[13] A. M. Garcia-Garcia and J. Wang, Phys. Rev. Lett. **94**, 244102 (2005); Phys. Rev. E **73**, 036210 (2006).

[14] J. Bourgain, M. Goldstein, and W. Schlag, Acta Math. **188**, 41 (2002); J. Bourgain, Ann. Math. **156**, 249 (2002); J. Anal. Math. **87**, 37 (2002).

[15] J. Bourgain, J. Anal. Math. **77**, 315 (1999); Commun. Math. Phys. **204**, 207 (1999); Lect. Notes Math. **1807**, 70 (2003).

[16] R. Blumel, S. Fishman, and U. Smilansky, J. Chem. Phys. **84**, 2604 (1986); R. Blumel and U. Smilansky, Phys. Rev. Lett. **52**, 137 (1984).

[17] G. Casati, I. Guarneri, and D. L. Shepelyansky, Phys. Rev. Lett. **62**, 345 (1989).

[18] J. Chabe, H. Lignier, H. Cavalcante, D. Delande, P. Szriftgiser, and J. C. Garreau, Phys. Rev. Lett. **97**, 264101 (2006).

[19] F. Borgonovi and D. L. Shepelyansky, Physica D **109**, 24 (1997).

[20] M. Schreiber and H. Grussbach, Phys. Rev. Lett. **76**, 1687 (1996); A. M. Garcia-Garcia and E. Cuevas, Phys. Rev. B **75**, 174203 (2007); M. Schreiber and H. Grussbach, Phys. Rev. Lett. **67**, 607 (1991); H. Aoki, J. Phys. C **16**, L205 (1983); A. MacKinnon and B. Kramer, Phys. Rev. Lett. **47**, 1546 (1981).

[21] E. Doron and S. Fishman, Phys. Rev. Lett. **60**, 867 (1988).

[22] J. T. Edwards and D. J. Thouless, J. Phys. C **5**, 807 (1972).

[23] B. I. Shklovskii, B. Shapiro, B. R. Sears, P. Lambrianides, and H. B. Shore, Phys. Rev. B **47**, 11487 (1993).

[24] V. E. Kravtsov and K. A. Muttalib, Phys. Rev. Lett. **79**, 1913 (1997); S. M. Nishigaki, Phys. Rev. E **59**, 2853 (1999).

[25] A. M. Garcia-Garcia, Phys. Rev. Lett. **100**, 076404 (2008).

[26] B. L. Altshuler, I. K. Zharekeshev, S. A. Kotochigova, and B. I. Shklovskii, Sov. Phys. JETP **67**, 62 (1988).

[27] D. Vollhardt and P. Wolfle, Phys. Rev. Lett. **48**, 699 (1982).

[28] M. Griniasty and S. Fishman, Phys. Rev. Lett. **60**, 1334 (1988); D. J. Thouless, *ibid.* **61**, 2141 (1988). D. Knuth, *Seminumerical Algorithms*, 2nd ed. (Addison-Wesley, Reading, MA, 1981).

[29] R. Blumel and U. Smilansky, Phys. Rev. Lett. **69**, 217 (1992).

[30] M. L. Mehta, *Random Matrices*, 2nd ed. (Academic Press, San Diego, 1991).

[31] E. Cuevas, Phys. Rev. Lett. **83**, 140 (1999); E. Cuevas, E. Louis, and J. A. Vergés, *ibid.* **77**, 1970 (1996).

[32] D. Braun, G. Montambaux, and M. Pascaud, Phys. Rev. Lett. **81**, 1062 (1998).

[33] A. M. Garcia-Garcia and J. Wang, Phys. Rev. Lett. **100**, 070603 (2008).